

Effective interatomic interactions in inhomogeneous semi-infinite systems

V. Drchal,* J. Kudrnovský,* L. Udvardi,† and P. Weinberger

Institute for Technical Electrochemistry, Technical University, Getreidemarkt 9, A-1060 Vienna, Austria

A. Pasturel

*Laboratoire de Thermodynamique et Physico-Chimie Metallurgiques, Domaine University,
38402 Saint Martin d'Hères, France*

(Received 1 October 1991)

The parameters entering the effective Ising model of disordered alloys with nonuniform composition at the sample surface are derived within the framework of the generalized perturbation method. The tight-binding version of the linear-muffin-tin-orbital method and its generalization to inhomogeneous alloys is used to describe the electronic structure in the local-density approximation, while the semi-infinite nature of the problem is included via the surface Green's-function approach. The method is applied to evaluate the site-diagonal terms of the Ising model as well as the effective interatomic interactions between sites within and between top layers up to the fourth-nearest neighbors of the fcc (001) face of the transition-metal alloys Pd₅₀Rh₅₀ and Ag₅₀Pd₅₀.

I. INTRODUCTION

Alloy phase stability in bulk solids, ordering and clustering phenomena, etc., are currently studied within a microscopic theory based on a generalized three-dimensional (3D) Ising model.¹ The problem consists of two equally important parts: (i) the quantum-mechanical description of the electronic structure, which supplies the parameters for the 3D Ising model; and (ii) the study of this model for $T > 0$, using methods of statistical mechanics.

The statistical part of the theory has already achieved a high level of sophistication. The traditional mean-field theory (Bragg-Williams approximation) is currently replaced by more advanced approaches. At present, the most important ones seem to be the cluster variation method² (CVM) and Monte Carlo simulations.³ In both approaches it is assumed that the configurationally dependent part of the internal energy can be written as a rapidly convergent sum of pair and multisite interatomic interactions.

The parameters entering the 3D Ising model are derived basically in two different ways. (i) A limited set (about ten) of periodic crystal structures representative for a given problem is chosen and their total energies are calculated within the local-density approximation (LDA). These energies are then directly mapped onto the Ising model. This method, proposed by Connolly and Williams,⁴ was recently developed further by Zunger and co-workers^{5,6} and is called the renormalized interaction approach (RIA). Standard *ab initio* band-structure techniques applied to suitably chosen small supercells can be used, and the double-counting terms are included. On the other hand, as the interaction energies, which are of order of a few mRy, are obtained as differences of total energies, the numerical requirements are severe. (ii) The multiple-scattering expansion of the thermodynamical potential for the statistically disordered alloy is the starting point for the generalized perturbation method (GPM)

of Ducastelle and Gautier,⁷ the concentration waves theory (CWT) of Gyorffy and Stocks,⁸ and the embedded cluster method (ECM) of Gonis *et al.*⁹ All these methods are based on the coherent-potential approximation (CPA) for the disordered state, and quite recently they were employed in calculations of the Ising model parameters from first principles.^{10,11} Here the advantages are explicit expressions for the interatomic interaction parameters and thus physical transparency. The double-counting terms are neglected on the basis of the so-called force theorem,¹² but further efforts to clarify this point would be desirable.

Very recently first attempts appeared to generalize the GPM theory also to the case of alloy surfaces. These studies^{13,14} are based on empirical tight-binding (TB) Hamiltonians and on the description of the semi-infinite solid in terms of a finite cluster of atoms using the recursion method.

The aim of this study is to present a systematic method for the calculation of the parameters for the 3D Ising model of semi-infinite disordered alloys, which can in turn be used as a starting point for a statistical treatment of surface-induced structural phenomena, such as segregation, ordering, and formation of other inhomogeneous patterns. The main parts of our method are (i) the application of the TB-LMTO (linear-muffin-tin-orbital) method to describe the electronic structure of the random alloy,¹⁵ (ii) the description of the semi-infinite geometry of the system within the surface Green's-function (SGF) formalism,¹⁶ (iii) the use of a CPA approach generalized to inhomogeneous systems,¹⁷ which allows us to describe any concentration profile connected with the surface, and (iv) the determination of the Ising Hamiltonian parameters within the GPM, using an expansion with respect to the inhomogeneous CPA effective medium.

II. THEORY

In order to determine the parameters of the Ising Hamiltonian for a semi-infinite disordered alloy with con-

centration inhomogeneities near the sample surface, one has to know its electronic structure. The corresponding formalism was developed recently.¹⁷ We therefore present here only those aspects necessary for the present purposes.

The semi-infinite alloy is considered to be divided into three parts: (i) a homogeneous bulk alloy, (ii) a (homogeneous) vacuum, e.g., represented by empty spheres with flat potentials, and (iii) an intermediate region consisting of several atomic layers, where all inhomogeneities (structural and electronic) of the system are concentrated, and which in the general case also contain a few layers of empty spheres. After configurational averaging, all layers could, at least in principle, have different local physical properties. To make the problem tractable, we assume that from a certain layer on the electronic properties of all subsequent layers are those of the corresponding infinite system, namely, either a homogeneous bulk

alloy, or the vacuum. We therefore approximate the semi-infinite alloy by an intermediate region that contains N atomic layers ($p = 1, 2, \dots, N$) and which is coupled to the vacuum and to the bulk alloy.

The central quantity to be determined is the configurationally averaged auxiliary resolvent¹⁵ of the system,

$$\bar{g}(z) = \langle [P(z) - S]^{-1} \rangle = [\mathcal{P}(z) - S]^{-1}. \quad (1)$$

Here, $P(z)$ is a site-diagonal potential function matrix, which characterizes the scattering properties of all sites. In a binary alloy $A_c B_{1-c}$ $P(z)$ is the site-diagonal potential function matrix, which at a given site R is randomly either $P^A(z)$ or $P^B(z)$. Within the CPA, the nonrandom, configurationally averaged coherent-potential function matrix $\mathcal{P}(z)$ is also a site-diagonal quantity.¹⁷

$$\mathcal{P}(z) = \begin{cases} \mathcal{P}_p(z), & p = 1, 2, \dots, N \text{ in the intermediate region} \\ \mathcal{P}^b(z) \text{ or } \mathcal{P}^v(z) & \text{otherwise,} \end{cases} \quad (2)$$

where the indices b and v refer to the bulk and vacuum region, respectively, and $\mathcal{P}^b(z)$ is determined using the bulk TB-LMTO-CPA method.¹⁵ For cubic lattices, studied in this work, $\mathcal{P}^b(z)$ is a diagonal matrix¹⁵ with respect to $L = (l, m)$. Due to the lowering of the symmetry at the surface, $\mathcal{P}_p(z)$ is nondiagonal with respect to L even for cubic lattices.¹⁷

In Eq. (1), S refers to the screened structure constants within the most localized nonrandom muffin-tin-orbital representation. The use of the screened structure constants has two important advantages. (i) As S is nonrandom by definition, and $P(z)$ is random, but site diagonal, the configurational average can be performed within the CPA. It should be noted that, contrary to the empirical TB-CPA method, no additional difficulties, such as off-diagonal randomness, arise. (ii) The short-range character of S allows us to introduce the concept of principal layers (PL), which greatly facilitates the theoretical treatment.

Within this concept, the semi-infinite alloy is viewed to be composed of PL's defined in such a way that only the nearest-neighboring PL's are coupled by the structure constants S . Depending on the actual structure of S , and on the face of the system, a PL consists of one or more atomic layers. For example, a restriction to first-(second-) nearest neighbors turns out to be sufficient^{16,18} for a fcc (bcc) lattice. Consequently, for a fcc (001), fcc (111), and bcc (110) surface, a PL is equivalent to just one atomic layer. For the sake of simplicity, in this paper we limit ourselves to this case. The generalization to the case of PL's consisting of more than one atomic layer is straightforward, and was developed previously.¹⁷

The coherent-potential matrices $\mathcal{P}_p(z)$ in the intermediate region, $1 \leq p \leq N$, are found from a set of coupled

inhomogeneous CPA equations which in matrix form is given by

$$\sum_{\alpha=A,B} c_p^\alpha t_p^\alpha(z) = 0, \quad (3)$$

$$t_p^\alpha(z) = [P^\alpha(z) - \mathcal{P}_p(z)] \{1 + \Phi_p(z) [P^\alpha(z) - \mathcal{P}_p(z)]\}^{-1}.$$

Here, the c_p^α are layer-dependent concentrations of the atoms $\alpha = A, B$ which are generally different from the bulk ones, $c_b^A = c$, and $c_b^B = 1 - c$. For a particular site R in a given layer p , $t_p^\alpha(z)$ and $\Phi_p(z)$ are the on-site elements of the single-site t matrix, and of the averaged resolvent \bar{g} , $\Phi_p(z) = \bar{g}_{R_p R_p}(z)$, respectively. To solve Eqs. (3), one needs an explicit expression for $\Phi_p(z)$. Due to the two-dimensional translational symmetry of $\bar{g}(z)$, one can perform a two-dimensional lattice Fourier transformation, by which the problem is reduced to a one-dimensional semi-infinite linear chain with nearest-neighbor interactions between PL's. The remaining step is now to determine the surface Green's function (SGF) of the bulk alloy and of vacuum. By definition, the SGF is the top PL projection of the resolvent of the semi-infinite homogeneous alloy or of the vacuum. These SGF's provide the necessary coupling to the intermediate region. In other words, using the concept of SGF's, one can reduce the original problem of infinite order to an effective problem of finite order N . By using bulk screened structure constants,

$$S_{pp}(k_{\parallel}) = S_{00}(k_{\parallel}),$$

$$S_{pq}(k_{\parallel}) = S_{01}(k_{\parallel}) \delta_{p+1,q} + S_{10}(k_{\parallel}) \delta_{p-1,q}$$

one gets for the (p, q) block ($1 \leq p, q \leq N$) of the inverse configurationally averaged resolvent $\bar{g}(k_{\parallel}, z)$

$$\{\bar{g}^{-1}(k_{\parallel}, z)\}_{pq} = [\mathcal{P}_p(z) - S_{00}(k_{\parallel}) - \Gamma_p(k_{\parallel}, z)]\delta_{pq} - S_{01}(k_{\parallel})\delta_{p+1,q} - S_{10}(k_{\parallel})\delta_{p-1,q}, \quad (4)$$

where

$$S_{pq}(k_{\parallel}) = \sum \exp\{ik_{\parallel}R\}S(R), \quad R \in \{R_{pq}\}. \quad (5)$$

Here, k_{\parallel} is a vector from the surface Brillouin zone and the symbol $\{R_{pq}\}$ denotes a set of vectors that connect one (arbitrarily chosen) site in the p th layer with all the sites in the q th layer. In Eq. (5) we made use of the fact that the structure constants S depend only on a difference vector $R = R_p - R_q$. In Eq. (4), $\Gamma_p(k_{\parallel}, z)$ denotes the coupling of the intermediate region to the alloy (or vacuum), namely,

$$\begin{aligned} \Gamma_1(k_{\parallel}, z) &= S_{10}(k_{\parallel})\mathcal{G}^v(k_{\parallel}, z)S_{01}(k_{\parallel}), \\ \Gamma_p(k_{\parallel}, z) &= 0 \quad \text{for } p=2, \dots, N-1, \\ \Gamma_N(k_{\parallel}, z) &= S_{01}(k_{\parallel})\mathcal{G}^b(k_{\parallel}, z)S_{10}(k_{\parallel}). \end{aligned} \quad (6)$$

The quantities $\mathcal{G}^{\lambda}(k_{\parallel}, z)$, $\lambda=v, b$ are the SGF's of the vacuum and of the homogeneous bulk alloy. They can be determined directly in real space by using the technique developed in Ref. 16, which avoids the k_{\perp} integration common to other approaches^{19,20} and reduces the problem to the following set of equations for $\mathcal{G}^b(k_{\parallel}, z)$ and $\mathcal{G}^v(k_{\parallel}, z)$:

$$\begin{aligned} \mathcal{G}^b(k_{\parallel}, z) &= [\mathcal{P}^b(z) - S_{00}(k_{\parallel}) \\ &\quad - S_{01}(k_{\parallel})\mathcal{G}^b(k_{\parallel}, z)S_{10}(k_{\parallel})]^{-1}, \\ \mathcal{G}^v(k_{\parallel}, z) &= [\mathcal{P}^v(z) - S_{00}(k_{\parallel}) \\ &\quad - S_{10}(k_{\parallel})\mathcal{G}^v(k_{\parallel}, z)S_{01}(k_{\parallel})]^{-1}, \end{aligned} \quad (7)$$

which has to be solved self-consistently. The layer-diagonal elements $\bar{g}_{pp}(k_{\parallel}, z)$ of the matrix $\bar{g}(k_{\parallel}, z)$ can be effectively calculated by a partitioning technique¹⁷ via a recursive set of equations terminated by Γ_1 and Γ_N [see Eqs. (6)]. The layer-diagonal-, but site-off-diagonal elements of $\bar{g}(z)$ are found from the expression

$$\bar{g}_{R_p R_p'}(z) = \frac{1}{N_{\parallel}} \sum_{k_{\parallel}} \bar{g}_{pp}(k_{\parallel}, z) \exp\{ik_{\parallel}(R_p - R_p')\}. \quad (8)$$

Here, N_{\parallel} is the number of lattice sites in a given layer. We remark that the quantity $\Phi_p(z)$ that enters the CPA equations (3) is a special case of Eq. (8), namely, $\Phi_p(z) = \bar{g}_{R_p R_p}(z)$. The layer-off-diagonal and site-off-diagonal elements of $\bar{g}(z)$, that enter the expressions for the Ising model parameters [see Eq. (15) below] can be found from (4) either by partitioning technique, or by direct inversion of $[\bar{g}(k_{\parallel}, z)]^{-1}$. For $\bar{g}_{R_p R_q}(z)$ one gets

$$\bar{g}_{R_p R_q'}(z) = \frac{1}{N_{\parallel}} \sum_{k_{\parallel}} \bar{g}_{pq}(k_{\parallel}, z) \exp\{ik_{\parallel}(R_p - R_q')\}. \quad (9)$$

This formally completes the solution of the electronic part of the problem.

The parameters of the semi-infinite alloy Ising Hamiltonian \mathcal{H}^I ,

$$\mathcal{H}^I = \mathcal{E}_0 + \sum_R \sum_{\alpha} \mathcal{D}_R^{\alpha} \eta_R^{\alpha} + \frac{1}{2} \sum_{R, R'} \sum_{\alpha, \alpha'} \mathcal{V}_{RR'}^{\alpha\alpha'} \eta_R^{\alpha} \eta_{R'}^{\alpha'} + \dots \quad (\alpha, \alpha' = A, \text{ or } B), \quad (10)$$

are the configurationally independent part of the alloy internal energy \mathcal{E}_0 , the on-site energy \mathcal{D}_R^{α} , the pair interatomic interactions $\mathcal{V}_{RR'}^{\alpha\alpha'}$, and, generally, the interatomic interactions of higher order. A particular configuration of the alloy is characterized by a set of occupation indices η_R^{α} , where $\eta_R^{\alpha} = 1$ if the site R is occupied by an atom of the type α , and $\eta_R^{\alpha} = 0$ otherwise. The parameters are found within the GPM by mapping at $T=0$ the grand-canonical potential $\Omega_{el}(T=0, E_F)$ of the electronic subsystem (where E_F is the Fermi energy)

$$\Omega_{el}(T=0, E_F) = - \int_{-\infty}^{E_F} N(E) dE \quad (11)$$

onto the Hamiltonian (10). The integrated density of states $N(E)$ for a particular configuration of the alloy is within the TB-LMTO-CPA formalism given by

$$N(E) = - \frac{1}{\pi} \lim_{\delta \rightarrow 0^+} \text{Im Tr} \left[\frac{1}{2} \ln \left[\frac{d}{dz} P(z) \right] + \ln[g(z)] \right], \quad (12)$$

where $z = E - i\delta$. The first term compensates the extra singularities in $\ln[g(z)]$, which originate from the poles of $P(z)$. In the most localized representation, as a rule, these singularities lie well outside the occupied part of the energy spectrum and need not be considered. Decomposing the configurationally averaged Green's function $\bar{g}(z)$ into its diagonal (\bar{g}_d) and off-diagonal (\bar{g}_{off}) parts with respect to lattice sites, one gets

$$\begin{aligned} \text{Tr} \ln g(z) &= \text{Tr}(\ln \bar{g}(z) - \ln\{1 + [P(z) - \mathcal{P}(z)]\bar{g}_d(z)\} \\ &\quad - \ln[1 + t(z)\bar{g}_{\text{off}}(z)]), \end{aligned} \quad (13)$$

where the quantities $P(z)$, $\mathcal{P}(z)$, and $t(z)$ are defined in Eqs. (1)–(3). The usual GPM expansion of Eq. (13) into multiple-scattering series yields for the Ising Hamiltonian parameters the expressions

$$d_R^{\alpha}(E) = \frac{1}{\pi} \lim_{\delta \rightarrow 0^+} \text{Im tr} \ln \{1 + [P_R^{\alpha}(z) - \mathcal{P}_R(z)]\bar{g}_{RR}(z)\}, \quad (14)$$

$$D_R^{\alpha}(E) = \int_{-\infty}^E d_R^{\alpha}(E') dE', \quad \mathcal{D}_R^{\alpha} = D_R^{\alpha}(E_F),$$

where $z = E - i\delta$. Similarly,

$$\begin{aligned} v_{RR'}^{\alpha\alpha'}(E) &= \frac{1}{\pi} \lim_{\delta \rightarrow 0^+} \text{Im tr} \ln [1 - t_R^{\alpha}(z)\bar{g}_{RR'}(z) \\ &\quad \times t_{R'}^{\alpha'}(z)\bar{g}_{R'R}(z)], \\ V_{RR'}^{\alpha\alpha'}(E) &= \int_{-\infty}^E v_{RR'}^{\alpha\alpha'}(E') dE', \quad \mathcal{V}_{RR'}^{\alpha\alpha'} = V_{RR'}^{\alpha\alpha'}(E_F), \end{aligned} \quad (15)$$

where Tr denotes the trace in configurational and angular momentum space, while tr means the trace over angular momentum space only. It is advantageous to rewrite the Ising Hamiltonian, Eq. (10), using the so-called transformation to the lattice gas model, $\eta_R^A = 1 - \eta_R^B = \eta_R$. If we limit ourselves to single-site and pair interactions, the Is-

ing Hamiltonian can be written up to a constant as

$$\mathcal{H}^I = \sum_R \mathcal{D}_R \eta_R + \frac{1}{2} \sum_{R,R'} \mathcal{V}_{RR'} \eta_R \eta_{R'}, \quad (16)$$

where

$$\mathcal{D}_R = \mathcal{D}_R^A - \mathcal{D}_R^B + \sum_{R'(\neq R)} [\mathcal{V}_{RR'}^{AB} - \mathcal{V}_{RR'}^{BB}], \quad (17)$$

$$\mathcal{V}_{RR'} = \mathcal{V}_{RR'}^{AA} + \mathcal{V}_{RR'}^{BB} - \mathcal{V}_{RR'}^{AB} - \mathcal{V}_{RR'}^{BA}. \quad (18)$$

The quantities $\mathcal{V}_{RR'}$ in (18) are the renormalized⁹ effective pair interactions (REPI); the unrenormalized⁷ ones (EPI) correspond to the first-order expansion of the logarithm in (15). Note that the sites R, R' are in general located in different layers p and q of the intermediate region. The corresponding energy-dependent quantities $V_{RR'}(E)$ and $v_{RR'}(E)$ are defined using the quantities $V_{RR'}^{\alpha\alpha'}(E)$ and $v_{RR'}^{\alpha\alpha'}(E)$ in (15) in analogy to (18). The quantity \mathcal{D}_R is the renormalized effective level or the point-cluster energy, which can contribute significantly to ordering and segregating processes in systems with inequivalent sites such as surfaces or bulk alloys with different sublattices. Note that according to (17), the on-site term \mathcal{D}_R is modified by pair interactions. Its energy-dependent counterpart $D_R(E)$ is obtained from $D_R^\alpha(E)$ and $V_{RR'}^{\alpha\alpha'}(E)$, Eqs. (14) and (15), in analogy to (17).

The multisite interatomic interactions can be evaluated similarly to the pair interactions. For example, for the unrenormalized triplet interactions one obtains in analogy with the EPI's

$$v_{RR'R''}^{\alpha\alpha'\alpha''}(z) \propto t_R^\alpha(z) \bar{g}_{RR'}(z) t_{R'}^{\alpha'}(z) \bar{g}_{R'R''}(z) t_{R''}^{\alpha''}(z) \bar{g}_{R''R}(z). \quad (19)$$

The energy-dependent quantities $V_{RR'R''}^{\alpha\alpha'\alpha''}(z)$ and $\mathcal{V}_{RR'R''}^{\alpha\alpha'\alpha''}$ are obtained in a similar manner. In analogy with the EPI's, it is common to work with effective triplet interactions (ETI) $\mathcal{V}_{RR'R''}$ defined as

$$\mathcal{V}_{RR'R''} = \{ \mathcal{V}^{AAA} - \mathcal{V}^{AAB} - \mathcal{V}^{ABA} - \mathcal{V}^{BAA} + \mathcal{V}^{ABB} + \mathcal{V}^{BAB} + \mathcal{V}^{BBA} - \mathcal{V}^{BBB} \}_{RR'R''}. \quad (20)$$

It should be noted that the ETI's modify both the on-site as well as the pair terms of the effective Ising Hamiltonian when the transformation to the lattice gas is performed.

III. RESULTS

The above formalism is applied to the (001) face of fcc $\text{Pd}_{50}\text{Rh}_{50}$ and $\text{Ag}_{50}\text{Pd}_{50}$ random alloys. Our choice is motivated by the fact that the PdRh system was studied for the bulk case both by the GPM method based on the KKR-CPA (Korringa-Kohn-Rostoker) method¹⁰ and using the renormalized interaction approach.^{5,6} We thus can compare our results for deep layers with the above-mentioned results. The system AgPd was studied by us previously,¹⁷ both for homogeneous and inhomogeneous concentration profiles at the sample surface. The PdRh system represents a weak-scattering limit of the alloy theory while the AgPd alloy exhibits a strong level disorder with non-negligible disorder in bandwidths.¹⁵

We mention briefly some details concerning the numerical part of the problem. We consider s, p , and d states

on each atom so that all occurring matrices are of order 9. For simplicity, we neglect the dependency of the potential functions $P^\alpha(z)$ on the layer index p , and use values derived from the self-consistent bulk TB-LMTO-CPA calculations. We also employ the simplest model for the vacuum-solid interface, namely, the hard-wall-like boundary condition.¹⁷ In this case, $\mathcal{G}^v(z)$ [see Eq. (6)] is simply zero. We have also made calculations with other types of boundary condition such as a step barrier, but the results for the PdRh system indicate that REPI's are not very sensitive to the actual form of the boundary condition. However, a further study of this point would be of interest.

The necessary Brillouin zone (BZ) integrations were performed over the full surface BZ [400 special k_{\parallel} points in a square surface BZ of the fcc (001) face]. All calculations were carried out in the complex energy plane and then analytically continued to the real axis. Note that the logarithms in Eqs. (14) and (15) should be evaluated from deconvoluted quantities.²¹ The set of coupled CPA equations (3) was solved for $N=3$, while the possible deviations from the bulk concentration were limited to the first two top sample layers.¹⁷ We have evaluated all REPI's up to the fourth-nearest neighbors (NN) within a given layer as well as between various layers in the surface near region. In order to compare our results with existing calculations for the bulk case,^{6,10} we have identified the first-, second-, and fourth-NN's in the fourth layer, and the third-NN between the third and fourth layers with the corresponding bulk alloy REPI values. Due to the fast convergence of the layer GF's to the bulk ones¹⁷ this is a very good approximation. We also evaluated some typical ETI's such as triangles and linear triplets in various top layers.

The REPI's for fcc (001) $\text{Pd}_{50}\text{Rh}_{50}$ alloy are summarized in Fig. 1. We note very good quantitative agree-

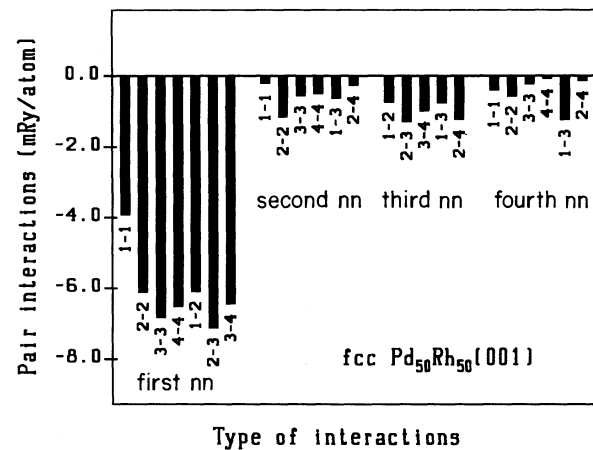


FIG. 1. Renormalized effective pair interactions for the fcc (001) $\text{Pd}_{50}\text{Rh}_{50}$ random alloy. The positions of atoms forming a pair are specified by layer indices p, q , whereby the index 1 refers to the surface, and by the type of neighbors (first- to fourth-nearest neighbors). The first-, second-, and fourth-nearest neighbors for $p=q=4$, and the third-nearest neighbors for $p=3, q=4$ can be identified with the corresponding bulk values.

ment of our results with those obtained for the bulk system.^{6,10} We also note the fast decrease of REPI's with distance in all layers including the surface layer. The negative values of REPI's indicate a strong tendency towards phase separation at $T=0$ which agrees with the existence of a miscibility gap in the bulk PdRh phase diagram. Note that contrary to a general conclusion made in Ref. 13 on the basis of a simplified model the first-NN surface REPI is not dominating. A similar effect was found recently also in the TiRh system.¹⁴

We have also compared the calculated REPI's with EPI's for Pd₅₀Rh₅₀ and Ag₅₀Pd₅₀ alloys. The general quantitative agreement is very good for both systems though our calculations for Pd₉₀V₁₀ system indicate non-negligible deviations.

In Table I we present the values of the ETI's calculated for the fcc (001) Ag₅₀Pd₅₀ alloy. We have chosen a few simple triplets, including various triangles and linear triplets along the [110] direction. The values of ETI's for triangles are generally very small as compared to the REPI's. For the bulk case this is in agreement with the results in Ref. 6. Similarly to the REPI's the ETI's also quickly approach the corresponding bulk values within a few layers below the surface. It is interesting to note that the largest ETI values are found for linear triplets, while the smallest values are obtained for triangles formed solely from nearest neighbors. This somewhat surprising result was also reported in the bulk alloy case.²²

The key to the understanding of the behavior of the REPI's lies in the energy-resolved quantities, $V_{RR'}(E)$, Eq. (15). They are shown in Figs. 2 and 3 for PdRh and AgPd alloys, respectively. Clearly, the actual value of the REPI depends strongly on E_F , or, alternatively, on the actual band filling. We note that for the PdRh system E_F lies between zeros of $V(E)$ thus indicating relative stability with respect to perturbations like the charge redistribu-

tion at the surface. This should be contrasted with situations when E_F lies close to the zeros of $V(E)$, especially those for the first-nearest neighbors. Such systems could be rather sensitive to a proper treatment of charge self-consistency, possible lattice relaxations, etc. Preliminary calculations indicate that the PdV system may be such a case. In accordance with the strong level disorder in AgPd mentioned above, the absolute values of the $V(E)$'s for the AgPd system are about three times larger than those for the PdRh system. Due to the position of E_F just above the d bands in Ag₅₀Pd₅₀, the absolute values of the REPI's are rather small. We note that for the AgPd system the values of the REPI's roughly follow the pattern predicted in Ref. 13.

In a statistical mechanical study of ordering or segregation phenomena at the surface on the basis of the Ising model (16) it is assumed¹³ that the REPI's do not depend on the actual concentration profile at the surface. In a proper treatment of the ordering and segregation processes both the REPI's and the concentration profiles should be determined in a self-consistent manner.¹⁴ In order to see how important modification of the REPI's due to the inhomogeneous concentration profile can be, we compare for fcc (001) Ag₅₀Pd₅₀ alloy¹⁷ in Fig. 4 the results of the homogeneous case with two inhomogeneous concentration profiles. We point out the following. (i) There is essentially no difference between the studied cases in the fourth layer. This, in turn, justifies our choice of the fourth layer as a "bulk" layer in the above analysis. (ii) The overall shape does not change dramatically in the alloy studied, nevertheless we find non-negligible differences for certain energies (i.e., for certain band fillings).

The values of the point-cluster energies may be decisive for the ordering or segregating phenomena in inhomogeneous systems, like alloy surfaces. In Fig. 5 we show

TABLE I. Effective triplet interactions (ETI) for the fcc (001) Pd₅₀Rh₅₀ random alloy. The positions of three atoms forming a cluster are specified by layer indices p_1, p_2 , and p_3 (index 1 refers to the surface layer) and by the type of neighbor pairs n_{12}, n_{23} , and n_{31} (indices 1, 2, and 4 refer to the first-, second-, and fourth-nearest neighbors).

p_1	p_2	p_3	n_{12}	n_{23}	n_{31}	ETI (mRy/atom)	Type
1	1	2	1	1	1	0.409	triangle
2	2	3	1	1	1	0.127	
3	3	4	1	1	1	0.081	
2	2	1	1	1	1	0.155	triangle
3	3	2	1	1	1	0.108	
4	4	3	1	1	1	0.087	
1	1	1	1	1	2	0.660	triangle
2	2	2	1	1	2	0.253	
3	3	3	1	1	2	0.200	
4	4	4	1	1	2	0.209	
1	1	1	1	1	4	0.649	linear triplet
2	2	2	1	1	4	0.980	
3	3	3	1	1	4	0.945	
4	4	4	1	1	4	0.962	

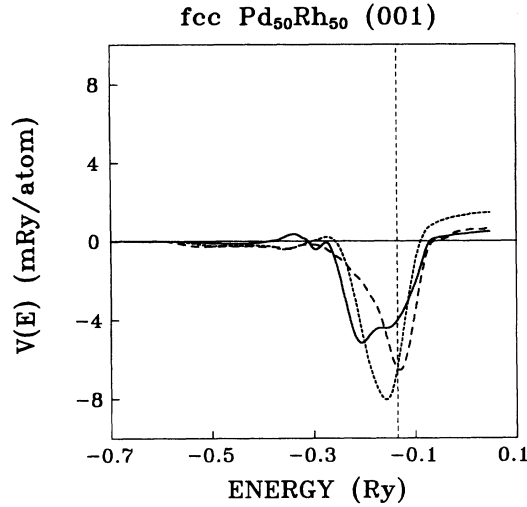


FIG. 2. Energy-resolved nearest-neighbor renormalized effective pair interactions $V_{R_p R'_q}(E)$ for the fcc (001) $\text{Pd}_{50}\text{Rh}_{50}$ random alloy. The full, dashed, and dotted lines denote the surface ($p=q=1$), the interlayer ($p=1, q=2$), and the bulk ($p=q=4$) terms, respectively. The dashed vertical line denotes the position of the bulk alloy Fermi level.

for the first top layers ($p=1,2,3$) the difference $D_p(E) - D_b(E)$ between the energy-resolved on-site terms and the value corresponding to the bulk (subscript b), represented by the fourth layer. As demonstrated in Ref. 13, this difference is roughly proportional to the difference in the surface tensions of the pure constituents. As an example we have chosen the case of the homogeneous $\text{Ag}_{50}\text{Pd}_{50}$ alloy. We have found a quick convergence of the point-cluster energies to their bulk value. Another

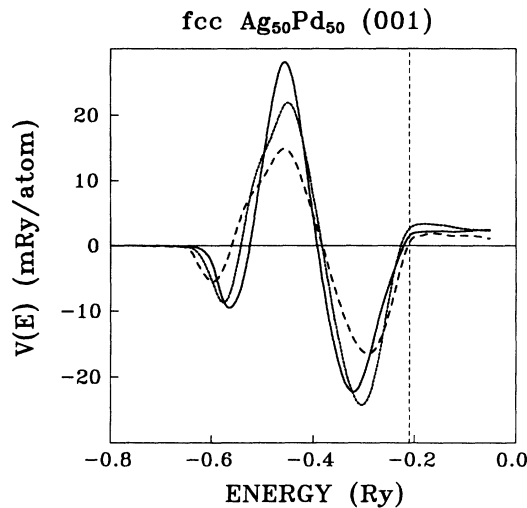


FIG. 3. Energy-resolved nearest-neighbor renormalized effective pair interactions $V_{R_p R'_q}(E)$ for the fcc (001) $\text{Ag}_{50}\text{Pd}_{50}$ random alloy. The full, dashed, and dotted lines denote the surface ($p=q=1$), the interlayer ($p=1, q=2$), and the bulk ($p=q=4$) terms, respectively. The dashed vertical line denotes the position of the bulk alloy Fermi level.

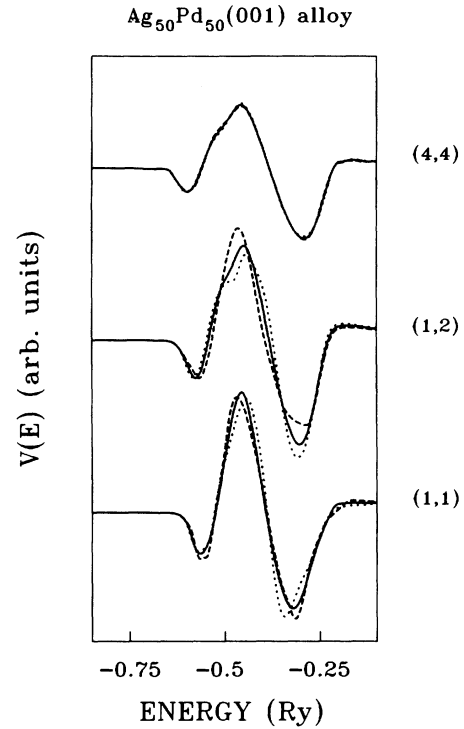


FIG. 4. Energy-resolved nearest-neighbor renormalized effective pair interactions $V_{R_p R'_q}(E)$ for fcc (001) AgPd random alloy with a bulk composition $\text{Ag}_{50}\text{Pd}_{50}$. We compare three concentration profiles $\text{Ag}_{c_1}\text{Pd}_{1-c_1}$ in the first two layers ($p=1,2$): (i) homogeneous profile, $c_1=c_2=0.5$ (full line), (ii) inhomogeneous profile, $c_1=0.1, c_2=0.75$ (dashed line), and (iii) inhomogeneous profile, $c_1=0.9, c_2=0.25$ (dotted line). The layer indices (p, q) of atoms forming a pair are attached to corresponding curves.

interesting result is that these differences may vary dramatically and even change sign. This may be quite important for segregation processes because the alloy can gain or lose energy when atoms in top layers are interchanged mutually.

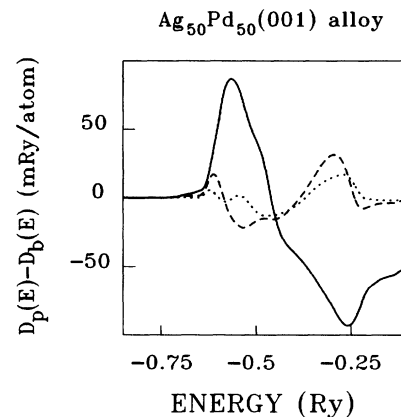


FIG. 5. Energy-resolved differences of the point-cluster energies, $D_p(E) - D_b(E)$, for the homogeneous fcc (001) $\text{Ag}_{50}\text{Pd}_{50}$ random alloy. The full, dashed, and dotted lines correspond to the first three layers, $p=1, 2, 3$, respectively.

IV. CONCLUSIONS

We have developed a method to calculate from first principles the parameters of the 3D Ising model of a random semi-infinite alloy with an arbitrary concentration profile near its surface. The generalized TB-LMTO-CPA technique¹⁷ is used to evaluate layer- and concentration-dependent effective levels and effective pair and triplet interatomic interactions of the Ising Hamiltonian within the GPM method. The numerical feasibility of the method was demonstrated for the cases of the fcc (001) faces of Pd₅₀Rh₅₀ and Ag₅₀Pd₅₀ alloys. For the case of deep layers we recovered the results obtained for the bulk alloy by other methods.^{6,10}

We have found important modifications of the pair interactions at the surface due to the changes in the local electronic structure, as well as due to the specific position of the bulk Fermi level dictated by the alloy composition. In agreement with similar studies based on empirical models,^{13,14} our calculations using the Bragg-Williams statistical model indicated a crucial importance of the on-site terms for the segregation process. We have found non-negligible modifications of the REPI's due to possible concentration-profile inhomogeneities at the surface. These modifications depend sensitively on the position of the bulk alloy Fermi level, i.e., on the band filling. Consequently, a consistent theory of surface segregation should include in each iteration step a recalculation of parameters of the effective Ising model for the concentra-

tion profile determined in the previous iteration from statistical mechanics.

The present version of the theory can be generalized in some respects, e.g., by including the effect of layer relaxation at the surface, by inclusion of the relativistic effects, and by considering other crystal faces. We mention at least two points which we think are of great importance for surface related problems and which should be clarified in the future: (i) the problems of charge self-consistency at the surface which lead to level shifts, and which can strongly modify on-site as well as interatomic parameters of the Ising model; and (ii) the problem of the double-counting terms neglected in the GPM-CPA method on the basis of the force theorem.¹²

Our method represents an approach based on the local-density approximation to construct the effective Ising Hamiltonian for alloy surfaces, which, in conjunction with the CVM approach or Monte Carlo simulations, opens a way to study surface alloy phase stability problems from first principles.

ACKNOWLEDGMENTS

This paper was supported by a grant by the Austrian Ministry of Science (Project Numbers GZ 45.123/4-II/A/4/90 and GZ 49.731/2-24/91) and by a grant of the Czechoslovak Academy of Sciences (Project Number 11015).

*Permanent address: Institute of Physics, Czechoslovak Academy of Sciences, Na Slovance 2, 180 40 Praha 8, Czechoslovakia.

†Permanent address: Institute of Physics, Technical University, Budafoki utca, 8, Budapest XI, Hungary.

¹For a review, see *Alloy Phase Stability*, Vol. 163 of *NATO Advanced Study Institute, Series E: Applied Sciences*, edited by G. M. Stocks and A. Gonis (Kluwer, Dordrecht, 1989).

²R. Kikuchi, *Phys. Rev.* **81**, 998 (1951); J. M. Sanchez, F. Ducastelle, and D. Gratias, *Physica A* **128**, 334 (1984); D. de Fontaine, in *Solid State Physics: Advances in Research and Applications*, edited by H. Ehrenreich, F. Seitz, and D. Turnbull (Academic, New York, 1979), Vol. 34, p. 73; C. Colinet, A. Bessoud, and A. Pasturel, *J. Phys. F* **18**, 903 (1988).

³K. Binder, in *Festkörperprobleme: Advances in Solid State Physics*, edited by P. Grosse (Vieweg, Braunschweig, 1986), Vol. XXVI.

⁴J. W. Connolly and A. R. Williams, *Phys. Rev. B* **27**, 5169 (1983).

⁵S.-H. Wei, L. G. Ferreira, and A. Zunger, *Phys. Rev. B* **41**, 8240 (1990).

⁶W. Lu, S.-H. Wei, and A. Zunger, *Phys. Rev. Lett.* **66**, 1753 (1991).

⁷F. Ducastelle and F. Gautier, *J. Phys. F* **6**, 2039 (1976).

⁸B. L. Gyorffy and G. M. Stocks, *Phys. Rev. Lett.* **50**, 374 (1983).

⁹A. Gonis, X. G. Zhang, A. J. Freeman, P. Turchi, G. M. Stocks, and D. M. Nicholson, *Phys. Rev. B* **36**, 4630 (1987).

¹⁰P. Turchi, G. M. Stocks, W. H. Butler, D. M. Nicholson, and A. Gonis, *Phys. Rev. B* **37**, 5982 (1988).

¹¹L. Szunyogh and P. Weinberger, *Phys. Rev. B* **43**, 3768 (1991).

¹²A. R. Mackintosh and O. K. Andersen, in *Electrons at the Fermi Surface*, edited by M. Springford (Cambridge University Press, Cambridge, England, 1980).

¹³G. Tréglia, B. Legrand, and F. Ducastelle, *Europhys. Lett.* **7**, 575 (1988); B. Legrand, G. Tréglia, and F. Ducastelle, *Phys. Rev. B* **41**, 4422 (1990).

¹⁴H. Dreyse, L. T. Wille, and D. de Fontaine, *Solid State Commun.* **78**, 355 (1991).

¹⁵J. Kudrnovský, V. Drchal, and J. Mašek, *Phys. Rev. B* **35**, 2487 (1987); J. Kudrnovský and V. Drchal, *ibid.* **44**, 7515 (1990).

¹⁶B. Wenzien, J. Kudrnovský, V. Drchal, and M. Šob, *J. Phys. Condens. Matter* **1**, 9893 (1989).

¹⁷J. Kudrnovský, B. Wenzien, V. Drchal, and P. Weinberger, *Phys. Rev. B* **44**, 4068 (1991); J. Kudrnovský, P. Weinberger, V. Drchal, *ibid.* **44**, 6410 (1991).

¹⁸O. K. Andersen and O. Jepsen, *Phys. Rev. Lett.* **53**, 2571 (1984); see also O. K. Andersen, O. Jepsen, and M. Šob, in *Electronic Band Structure and Its Applications*, edited by M. Yussouff (Springer-Verlag, Heidelberg, 1987), p. 1.

¹⁹W. R. L. Lambrecht and O. K. Andersen, *Surf. Sci.* **178**, 256 (1986).

²⁰H. L. Skriver and N. M. Rosengaard, *Phys. Rev. B* **43**, 9538 (1991).

²¹H. Eschrig, R. Richter, and B. Velický, *J. Phys. C* **19**, 7173 (1986).

²²K. Hirai and J. Kanamori, *J. Phys. Soc. Jpn.* **50**, 2265 (1984); A. Bieber and F. Gautier, *Z. Phys. B* **57**, 335 (1984). See also the review of F. Ducastelle in Ref. 1.